

Corrected holographic dark energy with power-law entropy and Hubble Horizon cut-off in FRW Universe

Vinod Kumar Bhardwaj¹, Priyanka Garg², Anirudh Pradhan³, Syamala Krishnannair⁴

^{1,2}Department of Mathematics, Institute of Applied Sciences & Humanities, GLA University, Mathura -281 406, Uttar Pradesh, India

³Centre for Cosmology, Astrophysics and Space Science (CCASS), GLA University, Mathura -281 406, Uttar Pradesh, India

⁴Department of Mathematical Sciences, Faculty of Science, Agriculture and Engineering, University of Zululand, Kwadlangezwa 3886, South Africa

¹E-mail: dr.vinodbhardwaj@gmail.com

²E-mail: pri.19aug@gmail.com

³E-mail: pradhan.anirudh@gmail.com

⁴E-mail: krishnannairs@unizulu.ac.za

Abstract

In the present work, we investigate the power-law entropy corrected holographic dark energy (PLECHDE) model with Hubble horizon cutoff. We use 46 observational Hubble data points in the redshift range $0 \leq z \leq 2.36$ to determine the present Hubble constant H_0 and the model parameter n . It represents a phase transition of the universe from deceleration to acceleration and has the transition point at $z_t = 0.71165$. We investigate the observational constraints on the model and calculate some relevant cosmological parameters. We examine the model's validity by drawing state-finder parameters that yield the result compatible with the modern observational data. The model's physical and geometrical characteristics are also explored, and they are shown to match well with current observations of observational Hubble data (OHD) and the latest joint light curves (JLA) datasets.

Keywords : PLECHDE, FRW metric, deceleration parameter, transit universe.

PACS: 98.80.-k

1 Introduction

We begin with the famous quote by Allan Sandage [1] that All the observational cosmological models are in search of two parameters: Hubble H_0 and deceleration parameters q_0 . The universe is a dynamic system in which its constituents (galaxies) travel like a disciplined march of soldiers and move away from each other with Hubble's rate. The recent astrophysical measurements of OHD (Observational Hubble data), SN Ia (Type Ia supernovae) [2, 3], CMBR (cosmic microwave background radiations) [4] anisotropy and Plank collaboration [5] indicated that our universe is expanding at faster rate. Mysterious dark energy (DE) [6, 7] is one of the

cause behind this accelerated expansion. According the prediction of CMBR, the universe is having flat geometrical shape on a large scale [8]. DE(dark energy) may be the cause of this flatness due to a lack of matter in the cosmos [9–12]. Many researchers have proposed various hypotheses to explain the occurrence of dark energy [13–17]. The Cosmological Constant (Λ) is thought to be the most effective DE option for describing the universe’s expansion. Various hypotheses have been developed to explain the nature of the cosmological constant [19–23].

Holographic dark energy (HDE) gets much attention from researchers from many proposed DE models. This is due to its direct relationship with space-time. This holographic dark energy supports in explanation of cosmic features of vacuum energy. It is normally accepted that the HDE models with the Hubble radius as the IR (Infra-red) cut-off do not follow the current cosmological accelerated expansion in FRW metric, while for the event horizon as the IR cut-off, cosmic acceleration of the universe exists [24]. Three popular HDE models, namely the Ricci scale, future event horizon, and Granda-Oliveros (GO) IR cut-offs, are investigated by Akhlaghi [25] showing the accelerated expansion and growth of the universe. In this direction, Ghaffari [26] examined the cosmological models of HDE with GO cut-off. In black hole thermodynamics, when the vacuum energy of a black hole is not greater than its mass, then Horizon length L is chosen as the IR cutoff. And the acquired vacuum energy is identified as HDE [27]. The holographic principle states that degrees of freedom are determined by bounding area rather than volume.

It should be noted that the entropy-area relationship of black holes affects the definition and derivation of holographic energy density ($\rho_D = 3c^2 \frac{M_p^2}{L^2}$). Following quantum effects influenced by Loop Quantum Gravity (LQG), the definition of the entropy-area relationship can be changed. When dealing with the entanglement of quantum fields in and out of the horizon, the power-law correction is a fascinating modification (correction) of the entropy-area $S(A)$ relation [28, 29].

The particular form of the power-law corrected entropy-area relation $S(A)$ is given as follows:

$$S(A) = c_0 \left(\frac{A}{a_1^2} \right) [1 + c_1 f(A)] \quad (1)$$

Here, $f(A)$ is considered by the power-law relation as

$$f(A) = \left(\frac{A}{a_1^2} \right)^{-\gamma} \quad (2)$$

where c_0 and c_1 are constants, a_1 is the UV cut-off at the horizon, and γ is a fractional power dependent on the degree of ground and excited state mixing. The contribution of the term $f(A)$ to the entropy $S(A)$ may be considered basically minor over a large horizon area (i.e., for $A \gg a_1^2$), and the mixed state entanglement entropy asymptotically approaches the ground state (Bekenstein-Hawking) entropy. The following relation may be used to produce the formulation of the entropy area relation $S(A)$ for power-law corrected entropy:

$$S(A) = \frac{A}{4G} (1 - K_\alpha A^{1-\alpha/2}) \quad (3)$$

with α is a dimensionless constant parameter, the constant K_α is considered as

$$K_\alpha = \frac{\alpha(4\pi)^{\alpha/2-1}}{(4-\alpha)r_c^{2-\alpha}} \quad (4)$$

The cross-over scale is indicated by the phrase r_c . Furthermore, we know that the quantity $A = 4\pi R_h^2$ suggest the horizon's area (with the horizon radius R_h). The second term in Eq. (3) gives the power-law correction to the entropy-area law. The entropy remains a well-defined quantity for positive value of parameter α i.e. ($\alpha > 0$). Inspired by the relation given in eq. (3), a new form of HDE (called the Power-Law Entropy-Corrected HDE (PLECHDE) [41, 42]) model was recently presented as follows:

$$\rho_D = 3n^2 M_p^2 L^{-2} - \beta M_p^2 L^{-\delta} \quad (5)$$

δ is a positive exponent, and β is a dimensionless parameter. The preceding equation provides the well-known holographic energy density in the exceptional case $\beta = 0$. The value of δ determines the significance of the corrected term in distinct locations. When $\delta = 2$, the two terms can be merged, recovering the standard HDE density. Let's look at the $\delta > 2$ and $\delta < 2$ cases independently. In the first situation, for $\delta > 2$, the corrected term can be comparable to the first term only when L is very small. The range of δ was claimed as $2 < \delta < 4$ [28]. On satisfaction of the generalized second law of thermodynamics for the universe with the power-law corrected entropy, the second situation $\delta < 2$ has been rejected [29]. Further, Sheykhi et al. [41] describe the Power-law entropy corrected holographic dark energy model for interacting and non-interacting scenarios.

Here, β is a dimensionless constant whose precise value need to be determined. Various authors have considered distinct value of the parameter β suitable for their cosmological models. Karami et al. [43] consider the value $\beta = -14.8$ to describe dynamics of agegraphic dark energy model. Karami and Abdolmaleki [44] have discuss the agegraphic dark energy model in $f(T)$ modified teleparallel gravity by assuming the values $\beta = 0.1, \beta = -10$ and $\beta = -14.8$. Recently, Jawad et al. [45] developed the Entropy corrected holographic dark energy models in modified gravity model utilizing $\beta = 0.5$. Following above mentioned analysis, we have described the dynamics of our model using the value $\beta = 0.001$.

The basic behaviour of the PLECHDE model with observational confrontation is investigated in this work. The authors discuss 28 observational Hubble observations in the region of redshift $0.07 \leq z \leq 2.3$, see in the reference [30]. For dark energy restrictions, Amirhashchi and Yadav [31] listed 31 $H(z)$ observations. To estimate the model parameter, Amirhashchi et al. [32] used 36 $H(z)$ data paired with JLA (Joint Light-curve Analysis) data. Goswami et al. [33] employed observational data from 38 $H(z)$ and 581 SN Ia. We employed 46 observational Hubble data points in the red-shift region $0 \leq z \leq 2.36$ in this work [34–37].

The objective of this described model is to consider Power-law entropy corrected Holographic dark energy by assuming IR cut-offs. Many cosmologists have proposed different parametrization of cosmological parameters, where the model parameters involved in the parametrization can be constrained by observational data, in order to describe certain phenomena of the universe, such as phase transition from early inflation era to late acceleration phase. We examine the Hubble parameter parametrization in the manner [38–40]: $H(a) = \alpha_1(1 + a^{-n})$; where $\alpha_1 > 0$ and $n > 0$ are constants. On integration of this parametrization, ewe get an explicit form of the scale factor as $a(t) = (c_1 e^{n\alpha_1 t} - 1)^{1/n}$; where $c_1 > 0$ is the constant of integration. The present explicit form of scale factor is an exponential function containing two model parameters n and α_1 which describe the dynamics of the universe. As $t \rightarrow 0$, we can have $a(0) = (c_1 - 1)^{1/n}$, which provides a non-zero initial value of scale factor for $c_1 \neq 1$ (or a cold initiation of universe

with finite volume). The manuscript is structured as: Section 2 presents the field equations of PLECHDE as IR cut-off. In Section 3, we proposed the solution of field equations. In Section 4, we describe an observational confrontation with recent $H(z)$ data on the model parameter. In subsections 5.1 and 5.2, we explain the behavior of deceleration parameter q versus redshift z and Statefinder, respectively. Finally, the conclusions are summarized in section 6.

2 Power law entropy corrected Holographic dark energy as IR cut-off

Homogeneous and anisotropic FRW metric form as

$$ds^2 = dt^2 - a^2(t)[dx^2 + dy^2 + dz^2] \quad (6)$$

where $a(t)$ is scale factor and function of t .

The Einstein's field equations (EFEs) in General Relativity (GR) can be written as:

$$R_j^i - \frac{1}{2}Rg_{ij} = -\frac{8\pi G}{c^4}(T_{ij} + \bar{T}_{ij}), \quad (7)$$

The energy momentum tensor for PLECHDE and matter for physical interpretation can be redefined as: $\bar{T}_{ij} = (\rho_\Lambda + p_\Lambda)u_i u_j + g_{ij}p_\Lambda$, where ρ_Λ and ρ_m represents PLECHDE and matter energy densities respectively, and p_Λ is the PLECHDE pressure.

The field equations for the discussed metric can be written as:

$$3\left(\frac{\dot{a}}{a}\right)^2 = \rho_m + \rho_\Lambda \quad (8)$$

$$\left(2\frac{\ddot{a}}{a} + \left(\frac{\dot{a}}{a}\right)^2\right) = -p_\Lambda, \quad (9)$$

The constants for the Einstein equations are assumed as $8\pi G = 1 = c$.

Taking IR cut-off as Hubble horizon, the power-law entropy corrected holographic dark energy (PLECHDE) is defined as:

$$\rho_\Lambda = 3c^2 M_p^2 H^2 - \beta M_p^2 H^\delta, \quad (10)$$

where $M_p^2 = \frac{1}{8\pi G}$ is the reduced plank constant and $3c^2$ is a numerical constant in the above relation. For $\delta > 2$, it was shown that the generalized second law of thermodynamics is conformed for the universe with power-law corrected entropy. As a result, the correction has a physical meaning only in the early cosmos, and it becomes meaningless as the universe grows larger [41].

3 Solutions of the field equations for PLECHDE

Type-Ia supernova observations [2, 3], WMAP (Wilkinson Microwave Anisotropic Probe) Collaboration [4] and Planck Collaboration [5], have been discussed about time-dependent DP which shows decelerating expansion in past, and accelerated expansion at present i.e. there is transition from decelerating to accelerating phase. So, to proposed an explicit solution for model of Universe, we have assumed a time dependent scale factor in the from

$$a(t) = (c_1 e^{n\alpha_1 t} - 1)^{\frac{1}{n}}, \quad (11)$$

where n , α_1 and c_1 are positive constants i.e. ($n > 0$, $\alpha_1 > 0$, $c_1 \neq 1$).

This scale factor suggest a model of transiting universe. The Hubble's and deceleration parameters are determined as

$$H = \frac{\dot{a}}{a} = \alpha_1 \left(\frac{c_1 e^{n\alpha_1 t}}{c_1 e^{n\alpha_1 t} - 1} \right) \quad (12)$$

$$q = -\frac{a\ddot{a}}{\dot{a}^2} = -\left(1 + \frac{\dot{H}}{H^2}\right) = -1 + \frac{n}{c_1 e^{n\alpha_1 t}} \quad (13)$$

Eq. (13) shows that the DP is time-dependent, which can take both positive and negative values representing early decelerating phase and later accelerating phase. From Eq. (13) we can see that $q = -1 + \frac{n}{c_1}$ as $t \rightarrow 0$, which is constant and positive for $n > 1$ and $c_1 < n$ and for $c_1 > n$, DP possesses negative value. This indicates that DP has a signature flipping nature from positive to negative era with the evaluation.

The scale factor and redshift z are linked by the relationship $a = \frac{a_0}{1+z}$. In terms of redshift z , we obtain the Hubble parameter defines as

$$H = \frac{H_0}{2} [1 + (1+z)^n], \quad (14)$$

Deceleration parameter is defined as

$$q = -\frac{\ddot{a}}{aH^2} = -1 + \frac{(1+z)}{H(z)} \frac{dH(z)}{dz}, \quad (15)$$

which is equivalent to

$$q = -1 - \frac{n(1+z)^{(n-1)}}{[1 + (1+z)^n]^2}, \quad (16)$$

From Eqs.(10) and (16), energy density of PLECHDE in term of redshift z

$$\rho_\Lambda = 3c^2 M_p^2 \left[\frac{H_0}{2} [1 + (1+z)^n] \right]^2 - \beta M_p^2 \left[\frac{H_0}{2} [1 + (1+z)^n] \right]^\delta, \quad (17)$$

We get matter energy density vs redshift z from Eqs. (8) and (16)

$$\begin{aligned}
\rho_m &= 3 \left[\frac{H_0}{2} (1 + (1+z)^n) \right]^2 - \rho_\Lambda \\
&= (1 + 3c^2 M_P^2) \left[\frac{H_0}{2} [1 + (1+z)^n] \right]^2 - \beta M_P^2 \left[\frac{H_0}{2} [1 + (1+z)^n] \right]^\delta.
\end{aligned} \tag{18}$$

The conservation for PLECHDE is expressed as $\dot{\rho}_\Lambda + 3H(\rho_\Lambda + p_\Lambda) = 0$. The equation of state (barotropic) is $p_\Lambda = \omega_\Lambda \rho_\Lambda$. Using Eq. (8), we find ω_Λ as :

$$\omega_\Lambda = -1 - \frac{\dot{H}}{3H^2} \frac{(6c^2 H^2 - \delta\beta H^\delta)}{(3c^2 H^2 - \beta H^\delta)} = -1 - \frac{2n}{3H_0} \frac{(1+z)^{n-1}}{(1+(1+z)^n)^2} \left[\frac{6c^2 - \delta\beta \left(\frac{H_0}{2}[1+(1+z)^n]\right)^{\delta-2}}{3c^2 - \beta \left(\frac{H_0}{2}[1+(1+z)^n]\right)^{\delta-2}} \right]. \tag{19}$$

4 Observational constraints on the model parameters

The observational data and statistical methodological analyses used to restrict the model parameters of the generated universe are presented in this section.

Hubble parameter $H(z)$

With the help of Hubble Space Telescope (HST) [46], Cepheid variable observations [47], gravitational lensing [48], and WMAP seven year data [49], many astrophysical researchers [50] estimated Hubble constant 72 ± 8 , $69.7_{-5.0}^{+4.9}$, 71 ± 2.5 , $70.4_{-1.4}^{+1.3}$, 73.8 ± 2.4 and 67 ± 3.2 . For more information, see Kumar [51], Sharma et al. [52], and Amirhashchi and Yadav [31]. For different redshifts, we consider an observed data set of 46 Hubble parameters H_{ob} with standard deviations σ_i .

In this section, we find constraints on the model parameter n by bounding the model under consideration with recent 46 points of $H(z)$ data set (OHD) in the redshift range $0 \leq z \leq 2.36$ with their corresponding standard deviation σ_i and compare with the Λ CDM model. The mean value of the model parameter n determined by minimizing the corresponding chi-square value, which is equivalent to the maximum likelihood analysis is given by

$$\chi_{OHD}^2(n) = \sum_{i=1}^{46} \frac{(H_{th}(n, z_i) - H_{ob}(z_i))^2}{\sigma(i)^2}. \tag{20}$$

Here, H_{th} and H_{obs} represent the theoretical and observed value of Hubble parameter H of our model and n is the model parameter.

Table 1: “The behaviour of Hubble parameter $H(z)$ with redshift

<i>S.No</i>	<i>Z</i>	<i>H(Obs)</i>	σ_i	References	<i>S.No</i>	<i>Z</i>	<i>H(Obs)</i>	σ_i	References
1	0	67.77	1.30	[53]	24	0.4783	80.9	9	[61]
2	0.07	69	19.6	[54]	25	0.48	97	60	[56]
3	0.09	69	12	[55]	26	0.51	90.4	1.9	[60]
4	0.01	69	12	[56]	27	0.57	96.8	3.4	[64]
5	0.12	68.6	26.2	[54]	28	0.593	104	13	[57]
6	0.17	83	8	[56]	29	0.60	87.9	6.1	[62]
7	0.179	75	4	[57]	30	0.61	97.3	2.1	[60]
8	0.1993	75	5	[57]	31	0.68	92	8	[57]
9	0.2	72.9	29.6	[54]	32	0.73	97.3	7	[62]
10	0.24	79.7	2.7	[58]	33	0.781	105	12	[57]
11	0.27	77	14	[56]	34	0.875	125	17	[57]
12	0.28	88.8	36.6	[54]	35	0.88	90	40	[56]
13	0.35	82.7	8.4	[59]	36	0.9	117	23	[56]
14	0.352	83	14	[57]	37	1.037	154	20	[57]
15	0.38	81.5	1.9	[60]	38	1.3	168	17	[56]
16	0.3802	83	13.5	[61]	39	1.363	160	33.6	[65]
17	0.4	95	17	[55]	40	1.43	177	18	[56]
18	0.4004	77	10.2	[61]	41	1.53	140	14	[56]
19	0.4247	87.1	11.2	[61]	42	1.75	202	40	[56]
20	0.43	86.5	3.7	[56]	43	1.965	186.5	50.4	[65]
21	0.44	82.6	7.8	[60]	44	2.3	224	8	[66]
22	0.44497	92.8	12.9	[59]	45	2.34	222	7	[67]
23	0.47	89	49.6	[61]	46	2.36	226	8	[68]”

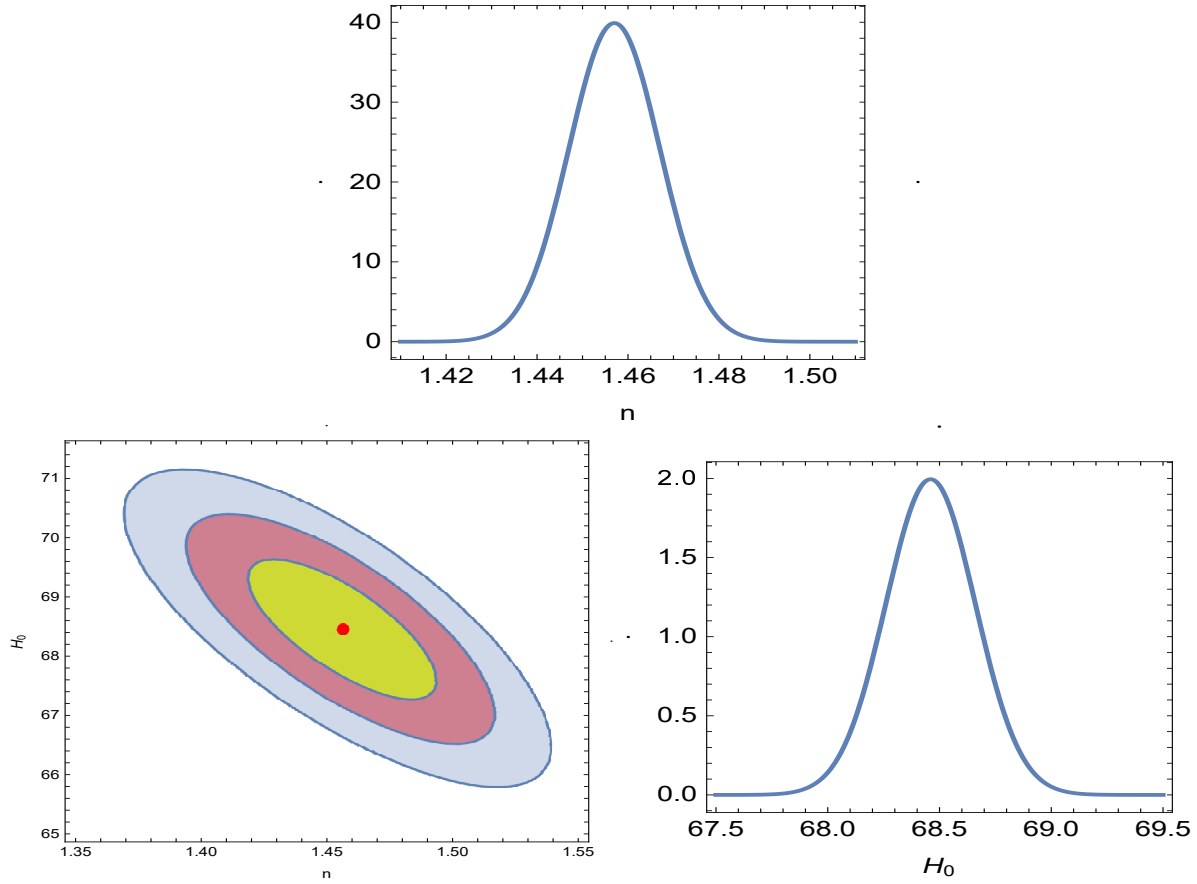


Figure 1: 1-Dimensional marginalized distribution and 2-Dimensional contour plots with best fitted values as $n = 1.457 \pm 0.037$ and $H_0 = 68.53 \pm 1.2$ in the $n - H$ plane.

Fig.1 shows the two dimensional contours with 68.3 %, 95.4 % and 99.7 % confidence level (CL) in $n - H$ plane. From figure, the best fit value of parameters are found as $n = 1.457 \pm 0.037$ and $H_0 = 68.53 \pm 1.2$.

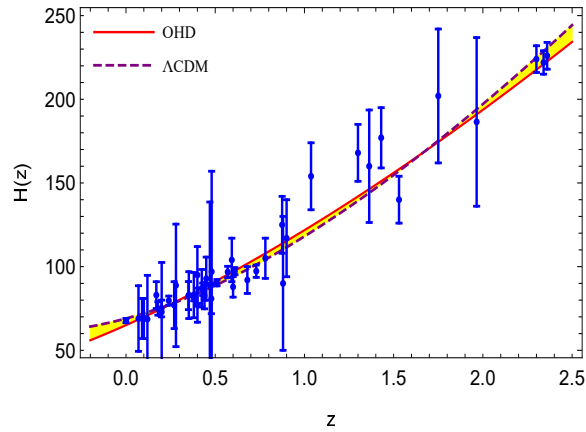


Figure 2: The behaviour of our model and the Λ CDM model with error bar plots of the Hubble data set.

Fig. 2 depicts the comparison of the best-fitting cosmological model of OHD data and Λ CDM with an error bar of Hubble data. We observe that graph for Λ CDM raise to a quite better fit. H increases with the increase of redshift z . Here dots signs are 46 observed values of the Hubble constant (H_{ob}). The best fit curve of the resulting model is represented by the solid red line, whereas the dashed black line represents the comparable Λ CDM model. It's worth noting that the resulting model's predicted value of H_0 closely matches the result of the Plank's collaboration [69].

5 Physical Behavior of Model

Here, we have discussed the physical properties of the cosmological model.

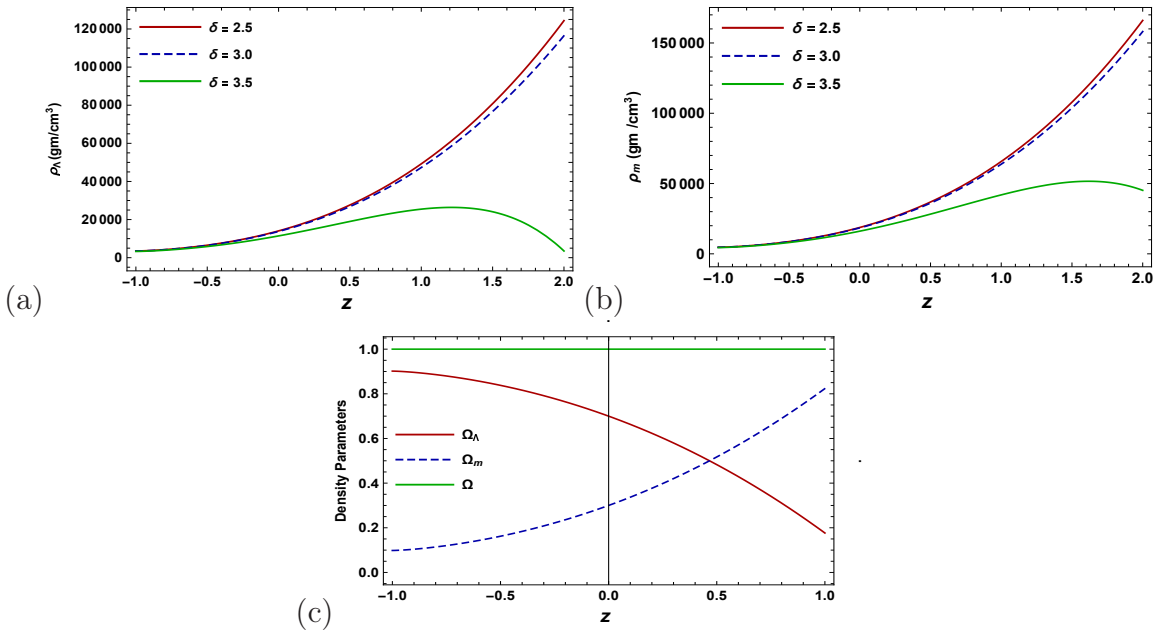


Figure 3: (a) Dark energy density vs redshift z with $\beta = 0.001$, $H_0 = 68.53$, $n = 1.457$, (b) Matter energy density vs redshift z with $\beta = 0.001$, $H_0 = 68.53$, $n = 1.457$, (c) Density parameters vs redshift z with $\beta = 0.001$, $\delta = 3.6092$, $H_0 = 68.53$, $n = 1.457$.

Figure 3(a) and its corresponding Eq. (17) portrays PLECHDE dark energy density (ρ_Λ) with IR cut-off versus redshift z for the observational values. It is found to be an increasing function of redshift z . For various estimations of δ , dark energy density ρ_Λ indicates the positive behavior throughout the evolution of the universe. Therefore we observe that our model is stable with recent observations.

Figure 3(b) shows matter energy density (ρ_m) versus redshift (z) for the observational values $n = 1.457 \pm 0.037$ and $H_0 = 68.53 \pm 1.2$. The figure shows that matter-energy density ρ_m increases slowly and leads to infinity. It is easy to see that the ρ_m is positive throughout the region and increases with redshift z for every different value of δ . This result is consistent with observations. Using the values $n = 1.457$, $\beta = 0.001$, and $H_0 = 68.53$, in Eq. (17), the δ is constrained as 3.6092 for the current observational value $\Omega_\Lambda = 0.7$. Figure 3(c) plots the variation of density parameters ($\Omega_\Lambda, \Omega_m, \Omega$) versus redshift z . From this figure, we observe that the ordinary matter dominates in the early universe, i.e., $\Omega_m > \Omega_\Lambda$, and it provides a strong

physical background for the earlier decelerating phase of the universe. But after a transition time, the density parameter for cosmological constant dominates the evolution, i.e., $\Omega_\Lambda > \Omega_m$ which is probably responsible for the accelerated expansion of the present-day Universe. The total density parameter (Ω) approaches 1 for a sufficiently large time, i.e., at the present epoch.

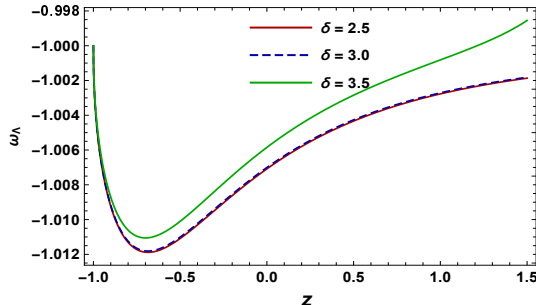


Figure 4: Plot of ω_Λ vs redshift z with $\beta = 0.001$, $H_0 = 68.53$, $n = 1.457$.

Figure 4 demonstrates the nature of the equation of state parameter ω_Λ concerning redshift z for PLECHDE. It is observed that the behavior of the EoS parameter is the same for all values of δ with the Hubble horizon cut-off. It is rapidly falling at the early stage while later on tends to constant value approximate -1.002 . We have also seen that it lies in phantom region ($\omega_D \leq -1$) for the observational parameters $n = 1.457 \pm 0.037$ and $H_0 = 68.53 \pm 1.2$. This result is consistent with the recent observational dataset.

5.1 Deceleration Parameter

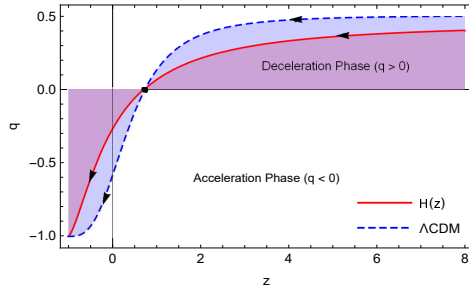


Figure 5: Plot of deceleration parameter q versus redshift z for both $H(z)$ and Λ CDM models.

Fig. 5 depicts the deceleration parameter comparing OHD and Λ CDM data. The solid red line exhibited the best fit curve of the derived model, and the dashed blue line displayed the corresponding Λ CDM model. The universe shows an expansion with the change of signature flipping from decelerating to accelerating phase at the transition redshift $z_t = 0.71165$. This transition redshift is well consistent with recent 36 OHD provided redshift range $0.07 \leq z \leq 2.36$ [33]. Comparing 740 SN Ia with JLA indicates a redshift range $0.01 \leq z \leq 1.30$. Thus our results are in good agreement with recent studies mentioned in Refs. [31–34].

5.2 Statefinder diagnosis

The statefinder pairs $\{r, s\}$ are the geometrical quantities that are directly obtained from metrics. This diagnostic is used to distinguish different dark energy models and hence becomes an

important tool in modern cosmology. Alam et al. [70] have defined the statefinder parameters r and s as following

$$r = \frac{\ddot{a}}{aH^3}, \quad s = \frac{r-1}{3(q-\frac{1}{2})} \quad (21)$$

A notable feature of the state finder is that these parameters are geometric because they depend on the scale factor and its time derivative [71]. In addition, different dark energy models show different evolutionary trajectories in the $s-r$ plane. In addition, the well-known flat Λ CDM model corresponds to points $s=0$ and $r=1$ on the $s-r$ plane. These properties of the Statefinder allow you to distinguish between different models of dark energy. In the literature, Statefinder diagnostic tools are often used to distinguish between different dark energy models [75, 76].

The statefinders can also read as

$$r = 2q^2 + q - \frac{\dot{q}}{H}, \quad s = \frac{2}{3}(q+1) - \frac{\dot{q}}{3H(q-\frac{1}{2})} \quad (22)$$

At $q = -1$, we observe as $r = 1$, $s = 0$ and our cosmic model resembles the Λ CDM model. For values of q in the range $-1 \leq q < 0.5$, we get the evolutionary $q-r$, $q-s$, and $s-r$ trajectories for the cosmological model, as illustrated in Figs. 6(a), 6(b), and 6(c). The flat Λ CDM model is shown by the black dot in panel (c) at $(s, r) = (0, 1)$. The Λ CDM statefinder pair $(0, 1)$ is an attractor in our cosmological model, which is interesting to note.

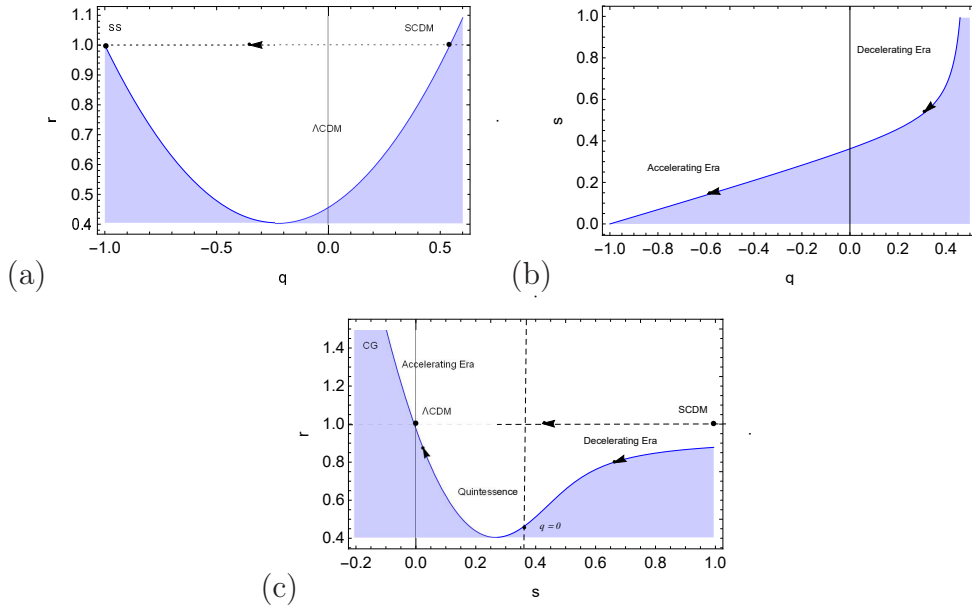


Figure 6: Plots of statefinders in $q-r$ plane (Fig.6a), $q-s$ plane (Fig.6b) and $s-r$ plane (Fig.6c). Here, black dot represents the location of point $(q, r) = (-1, 1)$ in the $q-r$ plane, $(q, s) = (-1, 0)$ and $(s, r) = (0, 1)$ in the $s-r$ plane. The vertical dashed line separates the acceleration and deceleration zones in the Fig.6a and Fig.6c. The arrows indicate the direction of trajectories' evolution as q varies from 0.5 to -1 .

6 Concluding Summary

In this paper, we have discussed the transition model of Power-law entropy corrected holographic dark energy in the context of Brans Dicke's theory. To find the solutions of the field equations, we have precised the energy density of PLECHDE $\rho_\Lambda = 3c^2 M_p^2 H^2 - \beta M_p^2 H^\delta$. We have also discussed the evolution of physical and dynamic parameters of the universe and their cosmological significance. The main highlights of the model are as follows:

- Figure 1, depicts one-Dimensional marginalized distribution and two-Dimensional contour plots with best fitted values as $n = 1.457 \pm 0.037$ & $H = 68.53 \pm 1.2$ in the $n - H$ plane.
- Figure 2 shows the comparison of the best-fitting cosmological model of OHD data and Λ CDM with the error bar of Hubble data. We observe that graph for Λ CDM raise to a quite better fit. H increases with the increase of redshift z . Here dots signs are 46 observed values of the Hubble constant (H_{ob}). It is worth noting that the derived model estimates H_0 are in good agreement with the Plank collaboration results [69].
- It has been observed from the figures 3(a) and 3(b) that for different values of δ , dark energy density ρ_Λ and matter energy density ρ_m are increasing function vs redshift z for the observational values $n = 1.457 \pm 0.037$ & $H = 68.53 \pm 1.2$.
- Plot 4, explain EoS parameter ω_Λ for the observational values for power law entropy corrected holographic dark energy. It has been plotted for three different values of δ (2.00, 2.05, 2.10). It is found to be negative and lies in phantom region ($\omega_D \leq -1$).
- Figure 5, explain of deceleration parameter q versus redshift z for both H(z) and Λ CDM models. In this derived model, it has been noted that PLECHDE model exhibits a smooth transition from deceleration to current acceleration phase at the transition point $z_t = 0.71165$. The filled circle shows the best fit values of the deceleration parameter at transition redshift. The results obtained in derived are consistent with observational data of modern cosmology, as clearly seen in fig.3.
- Figures 6(a), 6(b), and 6(c) show State-finders in the $q - r$ plane, $q - s$ plane, and $s - r$ plane. In the $q - r$ plane, the black dot represents SS and SCD models respectively, and in the $s - r$ plane, the black dot represents Λ CDM and SCDM models respectively. The vertical dashed line separates the acceleration and deceleration zones in the right and left panels. The arrows indicate the direction of trajectories' evolution as q varies from 0.5 to -1 . At $q = -1$, we notice that $r = 1$ and $s = 0$. As a result, at $q = -1$, our cosmological model resembles the Λ CDM model, which is consistent with current data.

Hence, our constructed transit PLECHDE model with observational data has good agreement with recent observations.

Acknowledgement

A. Pradhan thanks the IUCAA, Pune, India, for providing facilities under the associateship program. Sincere thanks are due to anonymous reviewers for their constructive comments to enhance the quality of the paper.

Appendix

From Eqs. (12) and (13), we obtain

$$H = \frac{\dot{a}}{a} \quad (23)$$

$$q = -\frac{a\ddot{a}}{\dot{a}^2} = -\frac{\dot{H}}{H^2} - 1 \quad (24)$$

The statefinders are defined as

$$r = \frac{\ddot{a}}{aH^3} = \frac{\ddot{H}}{H^3} + 3\frac{\dot{H}}{H^2} + 1 \quad (25)$$

Now from (24)

$$\frac{\ddot{H}}{H^3} = -\frac{\dot{q}}{H} + 2\frac{\dot{H}^2}{H^4} \quad (26)$$

Putting the values of (24) and (26) in Eq. (25), we get

$$r = -\frac{\dot{q}}{H} + 2\frac{\dot{H}^2}{H^4} - 3(q+1) + 1 \quad (27)$$

which reduces to

$$r = q(1+2q) - \frac{\dot{q}}{H} \quad (28)$$

From Eqs. (21) and (28), we obtain

$$s = \frac{r-1}{3(q-\frac{1}{2})} = \frac{2}{3}(q+1) - \frac{\dot{q}}{3H(q-\frac{1}{2})} \quad (29)$$

References

- [1] A.R. Sandage, Cosmology: A search for two numbers, *Physics Today* **23** (1970) 34.
- [2] S. Perlmutter, et al., Measurements of Ω and Λ from 42 high-redshift supernovae, *Astrophys. J.* **517** (1999) 565.
- [3] A.G. Riess, et al., Observational evidence from supernovae for an accelerating universe and a cosmological constant, *Astron. J.* **116** (1998) 1009.
- [4] D.N. Spergel, et al., First year wilkinson microwave anisotropy probe (WMAP) observations: Determination of cosmological parameters, *Astrophys. J. Suppl.* **148** (2003) 175.
- [5] P. De Bernardis, P.A.R. Ade, J.J. Bock, et al., A flat Universe from high-resolution maps of the cosmic microwave background radiation, *Nature* **404** (2000) 955.
- [6] A.G. Riess, et al., New Hubble space telescope discoveries of type Ia supernovae at $z > 1$: narrowing constraints on the early behavior of dark energy, *Astrophys. J.* **659** (2007) 98.
- [7] R. Jimenez, L. Verde, T. Treu, et al., Constraints on the equation of state of dark energy and the Hubble constant from stellar ages and the cosmic microwave background, *Astrophys. J* **593** (2003) 622.

- [8] M. Tegmark, et al., The three dimensional power spectrum of galaxies from the sloan digital sky survey, *Phys. Rev. D* **69** (2004) 103501.
- [9] T. Padmanabhan, Cosmological constant: the weight of the vacuum, *Phys. Rep.* **380** (2003) 235.
- [10] P.J.E. Peebles, B. Ratra, The cosmological constant and dark energy, *Rev. Mod. Phys.* **75** (2003) 559.
- [11] J. Martin, Quintessence: a mini-review, *Mod. Phys. Lett. A* **23** (2008) 1252.
- [12] S. Nojiri, S. D. Odintsov, Unified phantom cosmology: Inflation, dark energy and dark matter under the same standard, *Phys. Lett. B* **632** (2006) 597.
- [13] T. Chiba, T. Okabe, M. Yamaguchi, Kinetically driven quintessence, *Phys. Rev. D* **62** (2000) 023511.
- [14] T. Padmanabhan, T.R. Chaudhury, Can the clustered dark matter and the smooth dark energy arise from the same scalar field? *Phys. Rev. D* **66** (2002) 081301.
- [15] M.C. Bento, O. Bertolami, A.A. Sen, Chaplygin gas, accelerated expansion, and dark-energy-matter unification, *Phys. Rev. D* **66** (2002) 043507.
- [16] C.L. Bennett, et al., First year wilkinson microwave anisotropy probe (WMAP) observations: Preliminary maps and basic results, *Astrophys. J. Suppl.* **148** (2003) 1.
- [17] N. Bilic, G.B. Tupper, R. Viollier, Unification of dark matter and dark energy: the inhomogeneous chaplygin gas, *Phys. Lett. B* **535** (2002).
- [18] E. Komatsu, et al., Five-year wilkinson microwave anisotropy probe (WMAP) observations: cosmological interpretation, *Astrophys. J. Suppl.* **180** (2009) 330.
- [19] G. Hinshaw, et al., Five-year wilkinson microwave anisotropy probe observations: Data processing, sky Maps, and basic results, *Astrophys. J. Suppl.* **180** (2009) 225.
- [20] A.G. Riess, et al., Type Ia supernova discoveries at $z > 1$ from the Hubble space telescope: Evidence for past deceleration and constraints on dark energy evolution, *Astrophys. J.* **607** (2004) 665.
- [21] A.G. Riess, et al., New Hubble space telescope discoveries of type Ia supernovae at $z > 1$: narrowing constraints on the early behavior of dark energy, *Astrophys. J.* **659** (2007) 98.
- [22] J.M. Overduin, F.I. Cooperstock, Evolution of the scale factor with a variable cosmological term, *Phys. Rev. D* **58** (1998) 043506.
- [23] V. Sahni, A. Starobinsky, The Case for a positive cosmological Lambda-term, *Int. J. Mod. Phys. D* **9** (2000) 373.
- [24] W.J. Percival, C.M. Baugh, J. Bland-Hawthorn, et al., The 2dF galaxy redshift survey: the power spectrum and the matter content of the universe, *Mon. Not. Roy. Astron. Soc.* **327** (2001) 1297.

- [25] I.A. Akhlaghi et al., Model selection and constraints from holographic dark energy scenarios, *Mem. R. Astron. Soc.* **477** (2018) 3659.
- [26] S. Ghaffari, Holographic dark energy model in the DGP braneworld with time varying holographic parameter, *New Astron.* **67** (2019) 76.
- [27] M. Jamil, Variable G corrections to statefinder parameters of dark energy, *Int. J. Theor. Phys.* **49** (2010) 2829.
- [28] S. Das, S. Shankaranarayanan, S. Sourav, Power-law corrections to entanglement entropy of horizons, *Phys. Rev. D* **77** (2008) 064013.
- [29] N. Radicella, D. Pavon, The generalized second law in universes with quantum corrected entropy relations, *Phys. Lett. B* **691** (2010) 121.
- [30] Y. Chen, S. Kumar, B. Ratra, Determining the Hubble constant from Hubble parameter measurements, *The Astrophys. J.* **835** (2017) 86.
- [31] H. Amirhashchi, A.K. Yadav, Constraining an exact Brans-Dicke gravity theory with recent observations, *Phys. Dark Univ.* **30** (2020) 100711.
- [32] H. Amirhashchi, S. Amirhashchi, Constraining Bianchi type I universe with type Ia supernova and $H(z)$ data, *Phys. Dark Univ.* **29** (2020) 100557.
- [33] G.K. Goswami, et al., Two-fluid scenario in Bianchi type-I universe, *Mod. Phys. Lett. A* **35** (2020) 2050086.
- [34] V.K. Bhardwaj, A. Dixit, A. Pradhan, Bianchi type-V transitioning model in Brans-Dicke theory with observational constraint, arXiv:2203.11436[gr-qc] (2022).
- [35] A. Pradhan, V.K. Bhardwaj, P. Garg, S. Krishnannair, FRW cosmological models with Barrow holographic dark energy in Brans-Dicke theory, *Int. J. Geom. Method Mod. Phys.* (2022) 2250106. DOI: 10.1142/S0219887822501067.
- [36] A.K. Yadav, G.K. Goswami, A. Pradhan, S.K. Srivastava, Dark energy dominated universe in Lyra geometry, *Indian J. Phys.*, Accepted 1 March 2021. <https://doi.org/10.1007/s12648-021-02071-8>
- [37] V.K. Bhardwaj, A. Dixit, R. Rani, G.K. Goswami, A. Pradhan, An axially symmetric transitioning models with observational constraints, arXiv:2204.04451[gr-qc] (2022).
- [38] J.P. Singh, A cosmological model with both deceleration and acceleration, *Astrophys. Space Sc.* **318** (2008) 103.
- [39] N. Banerjee and S. Das, Acceleration of the universe with a Simple Trigonometric Potential, *Gen. Relativ. Grav.* **37** (2005) 1695.
- [40] S.K.J. Pacif et al., An accelerating cosmological model from a parametrization of Hubble parameter, *Mod. Phys. Lett. A* **35(5)** (2020) 2050011.
- [41] A. Sheykhi, M. Jamil, Power-Law entropy corrected holographic dark energy model, *Gen. Relative. Gravit* **43** (2011) 2661.

- [42] K. Karami et al., Holographic $f(T)$ -gravity model with power-law entropy correction, *Phys. Rev. D* **88** (2013) 084034.
- [43] K. Karami et al., Power-law entropy-corrected new agegraphic dark energy in Hořava–Lifshitz cosmology, *Can. J. of Phys.* **90** (2012) 473.
- [44] K. Karami, A. Abdolmaleki, $f(T)$ modified teleparallel gravity as an alternative for holographic and new agegraphic dark energy models, *Res. Astron. Astrophys* **13** (2013) 757.
- [45] A. Jawad, Abdul, N. Azhar, S. Rani, Entropy corrected holographic dark energy models in modified gravity, *Int. J. Mod Phys. D* **26** (2017) 1750040.
- [46] W.L. Freedman et al., Final results from the Hubble Space Telescope key project to measure the Hubble constant, *Astrophys. J.* **553** (2001) 47.
- [47] S.H. Suyu et al., Dissecting the gravitational lens B1608+ 656. II. Precision measurements of the Hubble constant, spatial curvature, and the dark energy equation of state, *Astrophys. J.* **711** (2010) 201.
- [48] N. Jarosik et al., Seven-year wilkinson microwave anisotropy probe (WMAP) observations: sky maps, systematic errors, and basic results, *Astrophys. J. Suppl.* **192**, 14 (2010).
- [49] A.G. Riess et al., A 3 % solution: determination of the Hubble constant with the Hubble Space Telescope and Wide Field Camera 3, *Astrophys. J.* **730**, 119 (2011).
- [50] F. Beutler et al., The 6dF Galaxy Survey: baryon acoustic oscillations and the local Hubble constant, *Mon. Not. R. Astron. Soc.* **416**, 3017 (2011).
- [51] S. Kumar, Observational constraints on Hubble constant and deceleration parameter in power-law cosmology, *Mon. Not. R. Astron. Soc.* **422**, 2532 (2012).
- [52] L.K. Sharma, B. K. Singh and A. K. Yadav, Viability of Bianchi type V universe in $f(R, T) = f_1(R) + f_2(R) + f_3(T)$ gravity, *Int. J. Geom. Methods Mod. Phys.* **17** (2020) 2050111.
- [53] E. Macaulay, et al., First cosmological results using Type Ia supernovae from the Dark Energy Survey: measurement of the Hubble constant, *Mon. Not. Roy. Astron. Soc.* **486** (2019) 2184.
- [54] C. Zhang, et al., Four new observational $H(z)$ data from luminous red galaxies in the Sloan Digital Sky Survey data release seven, *Res. Astron. Astrophys* **14** (2014) 1221.
- [55] J. Simon, L. Verde, R. Jimenez, Constraints on the redshift dependence of the dark energy potential, *Phys. Rev. D* **71** (2005) 123001.
- [56] D. Stern, et al., Cosmic chronometers: constraining the equation of state of dark energy. I: $H(z)$ measurements, *J. Cosmol. Astropart. Phys.* **1002** (2010) 008.
- [57] M. Moresco, et al., Improved constraints on the expansion rate of the Universe up to $z \sim 1.1$ from the spectroscopic evolution of cosmic chronometers, *J. Cosmol. Astropart. Phys.* **08** (2012) 006.

- [58] E. Gazta Naga, et al., Clustering of luminous red galaxies IV. Baryon acoustic peak in the line-of-sight direction and a direct measurement of $H(z)$, *Mon. Not. R. Astron. Soc.* **399** (2009) 1663.
- [59] D.H. Chuang, Y. Wang, Modelling the anisotropic two-point galaxy correlation function on small scales and single-probe measurements of $H(z)$, $DA(z)$ and $f(z)\sigma_8(z)$ from the Sloan Digital Sky Survey *DR7* luminous red galaxies, *Mon. Not. R. Astron. Soc.* **435** (2013) 255.
- [60] S. Alam, et al., The clustering of galaxies in the completed SDSS-III Baryon Oscillation Spectroscopic Survey: cosmological analysis of the DR12 galaxy sample, *Mon. Not. R. Astron. Soc.* **470** (2016) 2617.
- [61] M. Moresco, et al., A 6% measurement of the Hubble parameter at $z \sim 0.45$: direct evidence of the epoch of cosmic re-acceleration, *J. Cosmol. Astropart. Phys.* **05** (2016) 014.
- [62] C. Blake, et al., The WiggleZ Dark Energy Survey: joint measurements of the expansion and growth history at $z < 1$, *Mon. Not. R. Astron. Soc.* **425** (2012) 405.
- [63] A.L. Ratsimbazafy, et al., Age-dating luminous red galaxies observed with the Southern African Large Telescope, *Mon. Not. R. Astron. Soc.* **467** (2017) 3239.
- [64] L. Anderson, et al., The clustering of galaxies in the SDSS-III Baryon Oscillation Spectroscopic Survey: baryon acoustic oscillations in the Data Releases 10 and 11 Galaxy samples, *Mon. Not. R. Astron. Soc.* **441** (2014) 24.
- [65] M. Moresco, Raising the bar: new constraints on the Hubble parameter with cosmic chronometers at $z \sim 2$, *Mon. Not. R. Astron. Soc.* **450** (2015) L16.
- [66] N.G. Busca, et al., Baryon acoustic oscillations in the $Ly\alpha$ forest of BOSS quasars, *Astron. Astrophys.* **552** (2013) A96, arXiv:1211.2616 [astro-ph.CO]
- [67] T. Delubac, et al., Baryon acoustic oscillations in the $Ly\alpha$ forest of BOSS DR11 quasars, *Astron. Astrophys.* **584** (2015) A69.
- [68] A. Font-Ribera, et al., Quasar- $Ly\alpha$ forest cross-correlation from BOSS DR11: Baryon Acoustic Oscillations, *J. Cosmol. Astropart. Phys.* **2014** (2014) 027.
- [69] P. A. R. Ade et. al., Planck 2015 Results *XIII* cosmological parameters, *Astron. Astrophys.* **594** (2016) A13.
- [70] U. Alam, V. Sahni, T.D. Saini, A.A. Starobinsky, Exploring the expanding universe and dark energy using the Statefinder diagnostic, *Mon. Not. Roy. Astron. Soc.* **344** (2003) 1057.
- [71] V. Sahni, Exploring dark energy using the statefinder, arXiv:astro-ph/0211084 (2002).
- [72] A. Pradhan, A. Dixit, V.K. Bhardwaj, *Int. J. Mod. Phys. A*, **36** (2021) 2150030, arXiv:2101.00176[gr-qc].
- [73] A. Pradhan, V.K. Bhardwaj, A. Dixit, S. Krishnannair, A new class of holographic dark energy models in LRS Bianchi Type-I, *Int. J. Mod. Phys. A* **36** (2021) 2150256. arXiv:2203.05699[gr-qc].

- [74] A. Dixit, V.K. Bhardwaj, A. Pradhan, Barrow HDE model for Statefinder diagnostic in non-flat FRW universe, *Chinese J. Phys.* **77** (2022), 646-657, arXiv:2103.08339[gr-qc].
- [75] A. Ali, R. Gannouji, M. Sami, A.A. Sen, Background cosmological dynamics in gravity and observational constraints, *Phys. Rev. D* **81** (2010) 104029.
- [76] M. Malekjani, A. Khodam-Mohammadi, Statefinder diagnosis and the interacting ghost model of dark energy, *Astrophys. Space Sci.* **343** (2013) 451.